Proceedings of the International Workshop "Oxide Materials for Electronic Engineering" (OMEE-2009), Lviv 2009

Phase Transitions and Transport Properties of the Bismuth Vanadate-Based $(Bi,La)_4(V,Zr)_2O_{11-z}$ Ceramics

E.D. Politova[a,*], J.N. Torba[a], E.A. Fortalnova[a,b], G.M. Kaleva[a], M.G. Safronenko[b] and N.U. Venskovskii[b]

[a]Karpov Institute of Physical Chemistry, Vorontsovo Pole St., 10, 105064, Moscow, Russia

[b]Peoples' Friendship University of Russia, Ordzhonikidze St., 3, 117198, Moscow, Russia

Ceramic solid solutions $(Bi_{1-y}La_y)_4(V_{1-x}Zr_x)_2O_{11-z}$ with $x = 0$–0.05, $y = 0$–0.16 have been prepared by the solid state reaction method. The samples were studied by differential thermal analysis, X-ray diffraction, dielectric spectroscopy, and impedance methods. The concentration and temperature stabilization regions of the polymorphous α-, β-, γ'-, γ-modifications have been determined. The effects observed in dielectric properties, conductivity, and impedance data confirmed the influence both of intrinsic oxygen vacancies and those "pinned" at ferroelectric domain boundaries on the temperature hysteresis of α–β phase transition and their contribution to mechanism of oxygen ion transport.

PACS numbers: 64.60.−i, 72.20.−i, 77.22.Ch, 77.22.Gm

1. Introduction

Oxides on the base of bismuth vanadate $Bi_4V_2O_{11-y}$ reveal the highest ionic conductivity among other oxides. So, they are intensively studied as promising for pure oxygen generation [1, 2]. The parent bismuth vanadate compound undergoes phase transitions between α and β polymorphous modifications at approximately 700 K and between β- and tetragonal γ-phase at approximately 850 K [3–5]. Composition modifications by substitution of different valency cations for V^{5+} and/or Bi^{3+} cations were aimed at and succeeded in the stabilization of the tetragonal structure phase at the room temperature [6–19]. However, the poor thermodynamic stability of these oxides in reducing atmospheres hinders their real applications and comprises the main task to be solved. In this work, phase transitions and properties of ceramic solid solutions $(Bi_{1-y}La_y)_4(V_{1-x}Zr_x)_2O_{11-z}$ with $x, y < 0.2$, have been studied. By introduction of La^{3+} and Zr^{4+} cations, we intended to improve the thermodynamic stability of bismuth vanadate-based compositions.

2. Experimental procedure

Ceramic solid solutions $(Bi_{1-y}La_y)_4(V_{1-x}Zr_x)_2O_{11-z}$ with $x = 0$, 0.05, $y = 0.0$–0.16 were prepared by the solid state reaction method, starting from the preliminary dried oxides Bi_2O_3, V_2O_5, La_2O_3, ZrO_2 of high purity ($> 99.9\%$). Pressed pellets were calcined at 773–953 K (30 h), sintered at 1073 K (10 h), and slowly cooled.

The samples were analyzed using the X-ray diffraction (DRON-3M, Cu K_α radiation), differential thermal analysis (DTA) (MOM Q-1500 D), dielectric spectroscopy, and impedance methods (Agilent 4284 A LCR meter, 1 V) in the temperature range from 300 to 950 K and frequencies from 100 Hz to 1 MHz. Smaller flat surfaces of the samples used in electrical measurements were coated with Pt-containing paste and fired at 973 K.

3. Results and discussion

According to X-ray diffraction data, solid solutions based on $Bi_4V_2O_{11-z}$ are formed at $y \leq 0.08$ for $x = 0.0$ and at $y \leq 0.16$ for $x = 0.05$ (Fig. 1). In compositions with $x = 0.05$, $y > 0.08$, small peaks of admixture phases appear.

The monoclinic α-phase exists at $y \leq 0.05$ when $x = 0.0$ and only in the composition with $y = 0.0$ when $x = 0.05$. Transformation from orthorhombic β-phase to the tetragonal ordered γ'-phase takes place at $y \approx 0.11$, $x = 0.05$ (inset in Fig. 1, Fig. 2). At the room temperature, an increase in a, b, c unit cell parameters and the unit cell volume V is observed in the range of concentrations $0 \leq y \leq 0.06$. In compositions with higher y values, parameter a increases slightly, parameter b decreases slightly, while parameters c and V do not change with increasing concentration of La^{3+} cations. These results are consistent with the data obtained earlier for Zr- or La-doped bismuth vanadate solid solutions [6, 9, 10, 13–19].

The formation of solid solutions is supported by the DTA data (Fig. 3). Namely, shift of the DTA peaks confirms the influence of cation substitutions on tempera-

* corresponding author; e-mail: politova@cc.nifhi.ac.ru

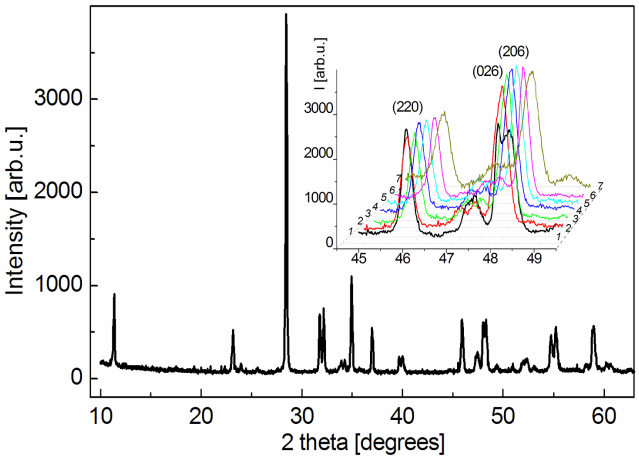

Fig. 1. The X-ray diffraction patterns of the $(Bi_{1-y}La_y)_4(V_{0.95}Zr_{0.05})_2O_{11-z}$ ceramics with $y = 0.0$. In inset, parts of the X-ray diffraction patterns for ceramics with $y = 0.0$ (*1*), 0.02 (*2*), 0.04 (*3*), 0.06 (*4*), 0.08 (*5*), 0.10 (*6*), 0.12 (*7*) are depicted.

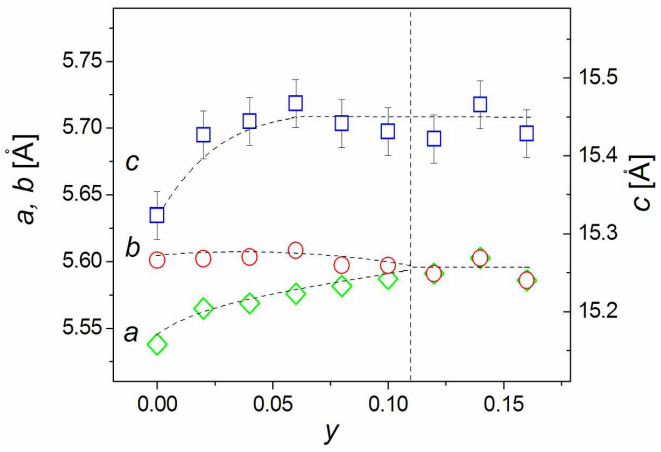

Fig. 2. Concentration dependences of the unit cell parameters a, b, c for $(Bi_{1-y}La_y)_4(V_{0.95}Zr_{0.05})_2O_{11-z}$ ceramics.

tures of phase transitions in solid solutions. According to DTA data, the presence of α–β and β–γ' reversible phase transitions is typical of the compositions studied (Fig. 3). In the DTA curves for the parent compound $Bi_4V_2O_{11-z}$, the first-order phase transitions are clearly seen. With increasing y value, temperature of α–β phase transition decreases sharply from 633 K to $<$ 290 K, while the temperature of the β–γ transition decreases from 807 K ($y = 0.0$) to 687 K ($y = 0.10$). Broadening of the β–γ phase transitions is typical of the compositions with $y > 0.08$. It is worse noting that the temperature hysteresis of β–γ phase transition increases from 36 K ($y = 0.0$) to 60 K ($y = 0.08$), always remaining smaller than the temperature hysteresis of α–β transition both in the samples with x, $y = 0.0$ (84 K) and with $x = 0.05$, $y = 0.0$ (98 K). It is believed that the main cause of such large temperature hysteresis of the α–β phase transition may be connected with the oxygen vacancies ordering–disordering in vanadium layers of the crystal structure and their "pinning" at the ferroelectric domain walls as well [18]. Samples with $x > 0.1$ which according to the X-ray data, have the ordered tetragonal γ'-structure at the room temperature are characterized by the reversible γ'–γ "order–disorder" phase transition at approximately 700 K.

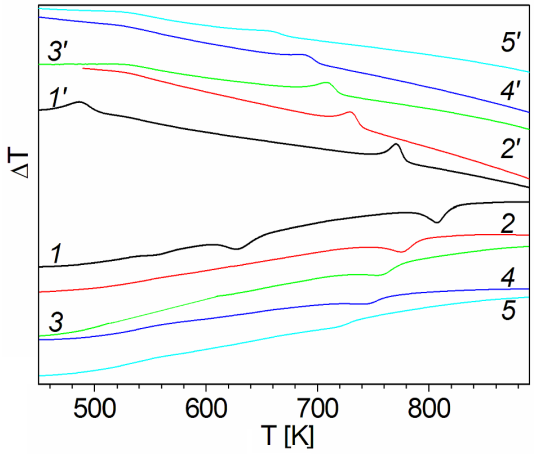

Fig. 3. DTA data for $(Bi_{1-y}La_y)_4(V_{0.95}Zr_{0.05})_2O_{11-z}$ ceramics solid solutions with $y = 0.0$ (*1, 1'*), 0.02 (*2, 2'*), 0.04 (*3, 3'*), 0.06 (*4, 4'*), 0.08 (*5, 5'*) measured on heating (*1–5*) and cooling (*1'–5'*).

In the dielectric permittivity $\varepsilon(t)$ and dielectric loss $\tan\delta(t)$ versus temperature plots, peaks, corresponding to ferroelectric-paraelectric α–β phase transition, were observed only for the samples with $x \leq 0.05$, $y \leq 0.05$ [14] (Fig. 4a, c, Fig. 5). Additionally, the effect of low temperature dielectric relaxation that is typical for ionic conductors was revealed in the orthorhombic β-phase ceramics (Fig. 4). In the $\sigma(1/T)$ curves, anomalies, corresponding to both α–β and β–γ phase transitions were also observed (Fig. 4b, d).

At the room temperature, the σ value of samples with $y = 0$ (α-phase) is higher by one order of magnitude than that of samples with $y = 0.1$ (ordered γ'-phase), though at 900 K, the σ value of samples which all have a disordered γ-phase structure changes by less than a half of an order of magnitude in the same concentration range.

This behavior may be indicative of the additional contribution of the ionic transport provided by the oxygen vacancies "pinned" at ferroelectric domain walls (or twin walls [20, 21]) to the common mechanism of fast ionic migration through vacant positions in the oxygen sublattice [22, 23] in the temperature domain of ferroelectric α-phase stability.

The impedance $Z''(Z')$ plots and $\tan\delta(f)$ spectra of both α- and β-phase compositions give additional support to these ideas. In the impedance $Z''/Z'(f)$ plots

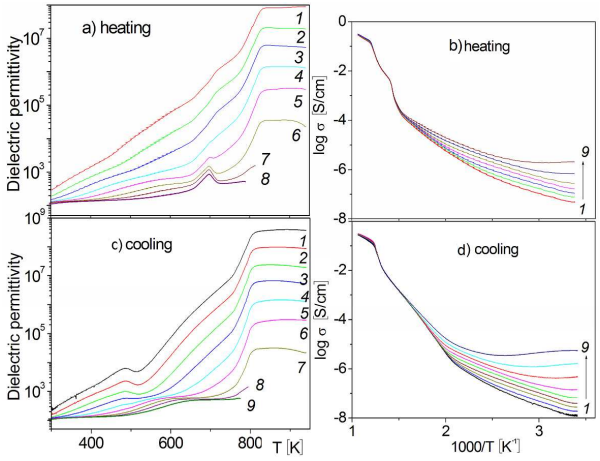

Fig. 4. Dielectric permittivity (a,c) and conductivity (b,d) versus temperature curves for $(Bi_{1-y}La_y)_4(V_{0.95}Zr_{0.05})_2O_{11-z}$ ceramic solid solutions with $y = 0.0$ measured on cooling and heating at frequencies of 100 Hz (*1*), 300 Hz (*2*), 1 kHz (*3*), 3 kHz (*4*), 10 kHz (*5*), 30 kHz (*6*), 100 kHz (*7*), 300 kHz (*8*), 1 MHz (*9*).

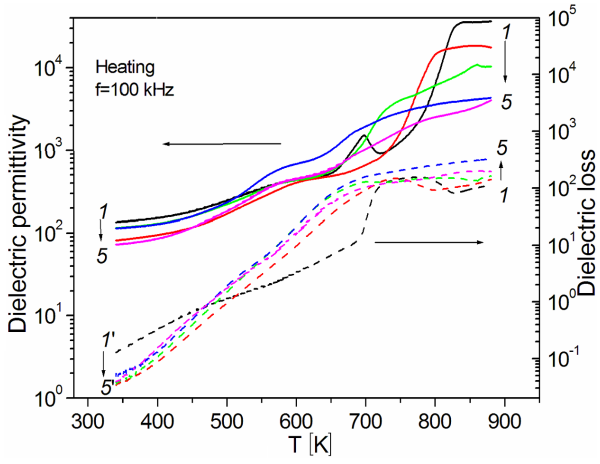

Fig. 5. Dielectric permittivity (solid) and dielectric loss (dash) versus temperature curves for $(Bi_{1-y}La_y)_4(V_{0.95}Zr_{0.05})_2O_{11-z}$ ceramic solid solutions with $y = 0.0$ (*1*), 0.02 (*2*), 0.04 (*3*), 0.06 (*4*), 0.08 (*5*) measured on heating at the frequency of $f = 100$ kHz.

pronounced semicircles were observed for both α- and β-phase compositions in the high frequency range at temperatures < 625 K (Fig. 6). The analysis of the impedance spectra obtained showed that deconvolution of grain–bulk and grain–boundary contributions from the total resistance was not possible. Additionally, two dielectric relaxation processes were revealed in dielectric loss versus frequency plots. Pronounced peaks were revealed in tan $\delta(f)$ plots at low and high frequencies, their frequency positions being dependent on the oxide compositions and measuring temperatures. At temperatures higher than ≈ 575 K, the contribution from charge transport across the electrolyte–electrode interface is clearly seen in the low frequency parts of the $Z''(Z')$ plots (Fig. 6, bottom).

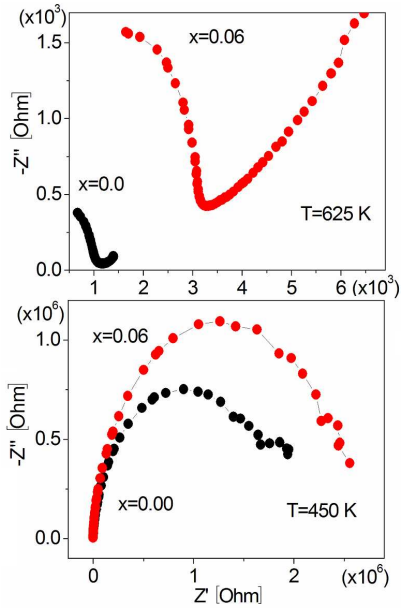

Fig. 6. Impedance $Z''(Z')$ plots for $(Bi_{1-y}La_y)_4(V_{0.95}Zr_{0.05})_2O_{11-z}$ ceramic solid solutions with $y = 0.0$ and $y = 0.06$ measured at 450 K (top) and 625 K (bottom).

4. Conclusions

The concentration and temperature stability regions of monoclinic α-, orthorhombic β- and tetragonal γ- and γ'-polymorph modifications were determined for ceramic solid solutions $(Bi_{1-y}La_y)_4(V_{1-x}Zr_x)_2O_{11-z}$ with $x = 0$ and 0.05, $y = 0.0$–0.16. The first-order α–β and β–γ reversible phase transitions were revealed in DTA curves, conductivity, dielectric permittivity and dielectric loss temperature dependences. The effects observed indicate that the crystal structure defects, such as intrinsic oxygen vacancies in the oxygen sublattice and those pinned at the domain/twin walls influence phase transitions and contribute to the mechanism of fast oxygen ion migration.

Acknowledgments

The financial support by the Russian Fund for Basic Research (grant 07-03-00133) is acknowledged.

References

[1] I. Abrahams, J.C. Boivin, G. Mairesse, G. Nowogrocki, *Solid State Ionics* **40/41**, 934 (1990).

[2] J.C. Boivin, C. Pirovano, G. Nowogrocki, G. Mairesse, Ph. Labrune, G. Lagrange, *Solid State Ionics* **113-115**, 639 (1998).

[3] A.A. Bush, Yu.N. Venevtsev, *Russ. J. Inorg. Chem.* **31**, 769 (1986).

[4] G. Mairesse, P. Roussel, R.N. Vannier, M. Anne, C. Pirovano, G. Novogrocki, *Solid State Sci.* **5**, 851 (2003).

[5] G. Mairesse, P. Roussel, R.N. Vannier, M. Anne, G. Novogrocki, *Solid State Sci.* **5**, 861 (2003).

[6] J. Yan, M. Greenblatt, *Solid State Ionics* **81**, 225 (1995).

[7] O. Joubert, M. Ganne, R.N. Vannier, G. Mairesse, *Solid State Ionics* **82**, 199 (1996).

[8] S.P. Simner, D. Suarez-Sandoral, J.D. Mackenzie, B. Dunn, *J. Am. Ceram. Soc.* **80**, 2563 (1997).

[9] A.A. Yaremchenko, V.V. Kharton, E.N. Naumovich, V.V. Samokhval, *Solid State Ionics* **111**, 227 (1998).

[10] W. Wrobel, I. Abrahams, F. Krok, A. Kozanecka, S.C.M. Chan, W. Bogusz, J.R. Dygas, *Solid State Ionics* **176**, 1731 (2005).

[11] C. Pirovano, M.C. Steil, E. Capoen, G. Novogrocki, R.N. Vannier, *Solid State Ionics* **176**, 2079 (2005).

[12] I. Abrahams, F. Krok, M. Malys, W. Wrobel, *Solid State Ionics* **176**, 2053 (2005).

[13] V.V. Murasheva, E.A. Fortalnova, E.D. Politova, M.G. Safronenko, S.Yu. Stefanovich, N.U. Venskovskii, *Mater. Sci. Forum* **587-588**, 114 (2008).

[14] E.A. Fortalnova, V.V. Murasheva, M.G. Safronenko, N.U. Venskovskii, S.Yu. Stefanovich, E.D. Politova, *Bull. Russ. Acad. Sci. Phys.* **72**, 1094 (2008).

[15] E.A. Fortalnova, V.V. Murasheva, M.G. Safronenko, N.U. Venskovskii, G.M. Kaleva, E.D. Politova, *Russ. J. Phys. Chem.* **82**, 1833 (2008).

[16] E.D. Politova, E.A. Fortalnova, G.M. Kaleva, S.Yu. Stefanovich, V.V. Murasheva, M.G. Safronenko, N.U. Venskovskii, P.B. Loginov, *Ferroelectrics* **367**, 8 (2008).

[17] E.D. Politova, E.A. Fortalnova, G.M. Kaleva, A.V. Mosunov, L.I. Andronova, S.A. Andropova, M.G. Safronenko, N.U. Venskovskii, *Phys. Solid State* **51**, 1443 (2009).

[18] A.A. Yaremchenko, V.V. Kharton, G.C. Mather, E.N. Maumovicha, F.M.B. Marques, *Bol. Soc. Esp. Ceram. Vidro* **38**, 635 (1999).

[19] E.D. Politova, E.A. Fortalnova, G.M. Kaleva, A.V. Mosunov, M.G. Safronenko, N.U. Venskovskii, V.V. Shvartsman, W. Kleemann, *Ferroelectrics* **391**, 3 (2009).

[20] C. Wang, Q.F. Fang, Y. Shi, Z.G. Zhu, *Mater. Res. Bull.* **36**, 2657 (2001).

[21] M. Kurumada, E. Iguchi, D.I. Savytskii, *J. Appl. Phys.* **100**, 014107 (2006).

[22] I. Abrahams, F. Krok, *J. Mater. Chem.* **12**, 3351 (2002).

[23] I. Abrahams, F. Krok, *Solid State Ionics* **157**, 139 (2003).